Experimental Heat Transfer, vol. 2, pp. 237–255, 1989

MEASUREMENT TECHNIQUES FOR HORIZONTAL FLOW BOILING HEAT TRANSFER WITH PURE AND MIXED REFRIGERANTS

D. S. Jung
Department of Mechanical Engineering, University of Maryland, College Park, Maryland 20742

M. McLinden
Center for Building Technology, National Institute of Standards and Technology, Gaithersburg, Maryland 20899

R. Radermacher
Department of Mechanical Engineering, University of Maryland, College Park, Maryland 20742

A test rig and measurement techniques for horizontal flow boiling of pure and mixed refrigerants are described. Local heat transfer coefficients were measured for R22/R114 and R12/R152a mixtures as well as the corresponding pure components. The test section consists of an 8-m-long, 9.1-mm-i.d., electrically heated stainless steel tube and has the distinctive feature of variable heated length. Details of pressure, composition, and fluid and wall temperature measurements are discussed. The composition of subcooled liquid entering test section varied from test to test, and it is recommended that it be measured for each test. For the R22/R114 mixture, local composition measurements in the annular liquid film revealed a composition variation of up to 0.07 mole fraction around the circumference of the heated tube.

INTRODUCTION

For the past few decades, much work has been directed toward an understanding of the boiling process with pure substances. Thanks to these efforts, many aspects of boiling heat transfer with pure substances are well explored at present. Addition of another component to a pure substance, however, increases the number of variables, which makes boiling processes with mixtures much more complicated. Due in part to this complexity, boiling heat transfer with mixtures has received considerably less attention than that with pure fluids. The lack of general correlations for boiling heat

This work was funded by the Electric Power Research Institute (Project No. RP8406-2, under the supervision of Dr. Jong Kim, Project Manager) and the National Institute of Standards and Technology (NIST) and was carried out in the laboratories of NIST. The authors would like to acknowledge the many helpful discussions with D. Didion at NIST and H. Ross at NASA Lewis Research Center. We wish to thank Professors Yong Chul Cho and Chong Bo Kim at Inha University, Incheon, Korea, for their constant encouragement during the course of this study.

NOMENCLATURE

A	heat transfer area, m^2	X	equilibrium liquid composition
C_p	specific heat, kJ/kg K	Y	equilibrium vapor composition
d	diameter, m		
G	mass flux, kg/m^2 s	Subscripts	
h	heat transfer coefficient, W/m^2 K	b	bottom
k	thermal conductivity, w/m K	eq	equilibrium
$\dot{m}$	mass flow rate, g/s	f	fluid
p_r	reduced pressure	l	liquid
Q	power input, w	tp	two-phase
q	heat flux, W/m^2	v	vapor
T	temperature, K or °C	w	wall

transfer in mixture systems, especially in convective boiling heat transfer, is now one of the limitations in the design of efficient evaporation equipment [1].

Recently, the use of nonazeotropic refrigerant mixtures as working fluids in heat pumps has shown theoretical promise, which has been verified experimentally [2]. Studies in an experimental heat pump have demonstrated an increase in the coefficient of performance of up to 32% for an optimized mixed refrigerant as compared to the performance of pure R22 [2]. Several other advantages have been claimed for nonazeotropic mixtures in refrigeration systems. Among these are improved thermodynamic efficiency; lower pressure ratios across the compressor; and the ability to change refrigerant composition, allowing the working medium's capacity to match load requirements.

Despite these advantages, however, the use of refrigerant mixtures in heat pumps has not yet been popular due in part to the lack and inaccuracy of such design data as heat transfer coefficients. As discussed by Kenning and Hewitt [3], careful measurements are essential in order to provide the reliable data necessary to develop general heat transfer correlations for both pure and mixed fluids. Of particular concern in this study are the measurement techniques for flow boiling heat transfer in a horizontal geometry for both pure and mixed refrigerants.

In 1983, Singal et al. [4] reported the horizontal flow boiling heat transfer coefficients obtained from a R13/R12 mixture. Their test section was composed of two identical horizontal stainless steel tubes, each of which is 2.35 m long, 9.52 mm i.d., and 3 mm thick. These tubes were connected by a smooth U-turn bend. Three thermocouples were spot-welded on the top, side, and bottom of the tube. A backpressure-regulating valve was used to maintain a constant pressure at the outlet of the test section. The composition of R13 was 0-20% by mass in increments of 5%. They, however, did not measure heat transfer coefficients for pure R13. Their wall temperature profiles showed large scatter along the channel. They found that average heat transfer coefficients for the binary mixtures were slightly greater than those for pure R12.

Ross et al. [5] conducted a series of experiments with an R13B1/R152a mixture having overall compositions of 0.07, 0.22, 0.36, and 0.64 mole fraction R13B1. Their test section was composed of a 2-m-long preheating section and a 0.7-m-long main test section. By varying the heat flux in the preheating section, qualities available in the

main test section could be adjusted, which enabled data in a wide range of qualities to be obtained in the main test section. This, however, required huge efforts to cover a wide range of qualities.

Four and five wall thermocouple groups were attached on the preheating and test section, respectively. Each group had four copper-constantan thermocouples, which were clamped at the top, sides, and bottom of the tube and electrically isolated from the test section by a thin layer of PTFE (Teflon) tape. The outlet pressure was kept at 480 kPa during the tests. For the analysis of data, all thermodynamic properties of pure and mixed refrigerants were calculated by the Carhahan-Starling-DeSantis (CSD) equation of state [6]. The results revealed a substantial degradation of heat transfer coefficients for an R13B1/R152a mixture in the nucleate boiling-dominated regime.

Ross et al. [5] also reported for the first time a circumferential variation of wall temperatures with mixtures in annular flow. For pure components, the wall temperature at the bottom of the tube was higher than that at the top. For mixtures, however, a new phenomenon, opposite pure component behavior, was observed: The wall temperature at the bottom was lower than that at the top. This unique phenomenon was also seen partly in Singel et al.'s data [4], but they could not identify it due to large wall temperature fluctuations. Ross et al. conjectured that the cause for this phenomenon might be a composition variation around the circumference of the heated tube; they, however, did not attempt to measure any such composition variation.

Recently, Kenning and Hewitt [3] measured heat transfer coefficients for water in horizontal annular flow boiling at 160 and 390 kPa in a 9.6-mm-bore cupronickel tube. They described the difficulty of measuring local pressures over a long period and demonstrated a few methods to measure local pressures to compute corresponding saturation temperatures accurately. The measurement of local pressure was found to be the most likely source of discrepancies among many studies. They also observed a significant thermal entry-length effect on heat transfer under certain conditions and suggested that data from systems with a very short heated length such as Bennett's [7] should not be used for the development of general heat transfer correlations.

From a survey of related experimental efforts [1, 3–5, 7], it becomes clear that the following points should be emphasized in the measurements of flow boiling heat transfer coefficients for both pure and mixed refrigerants:

1. Construction of a long test section to eliminate entry-length effects and to facilitate measurements over a wide range of vapor qualities
2. Accurate wall temperature, local pressure, and composition measurements
3. Examination of a variety of working fluids using the same test section and instrumentation to eliminate any inconsistency in data analysis
4. Accurate error analysis to ascertain the reliability to the data

The primary purpose of this paper is to discuss the problems encountered in previous measurements, to suggest experimental techniques to overcome them, and finally to discuss the results qualitatively. Detailed analysis and correlation of the horizontal flow boiling heat transfer data for both pure and mixed refrigerants, obtained by using the experimental techniques discussed below, are available elsewhere [8, 9].

EXPERIMENTS

Experimental Apparatus

Figure 1 shows the schematic diagram of the test rig. A semihermetic, oil-free pump delivers subcooled liquid refrigerant to the test section. Just before the test section inlet, a calibrated turbine flow meter and a flow regulating valve are installed to measure and control the flow rate. The subcooled liquid is heated by passing a DC current through the tube. The vapor generated in the test section is condensed in the condenser, which is cooled by brine at -20 to -60C. The pump then draws the liquid from the bottom of the condenser to complete the cycle. The flow patterns were observed through sight glasses installed before and after the test section. In order to reduce the heat gain (or loss) from (or to) the surroundings, the test section was covered with 200-mm-diameter fiberglass insulation.

The test section was made of two identical 4-m-long, 9.1-mm-i.d., type 304 stainless steel tubes (specification ASTMA 269/213) with a nominal wall thickness of 0.25 mm. The tolerances of diameter and wall thickness are 0.127 mm and 10% of the nominal wall. The thermal conductivity of the tube is 14 ± 2 W/m K at room temperature. Due to space limitations, these two sections were connected by a 180° U-turn bend, made of coper tube with a similar inside diameter. The test section was rigidly attached to the frame near the condenser side but was otherwise free to move axially due to thermal expansion (or contraction). It was electrically isolated from the fram and the U-turn bend by using plastic bushings at the ends.

There are three bus connections to the DC power supply on the first 4-m section and five on the second 4-m section. These bus connections effectively created a variable-length test section, which is one of the distinctive features of the current test rig. For instance, for high heat flux and low mass flow rate, only a part of the 8-m length was heated to yield the exit quality of up to 80–90%. For low heat flux and high mass flow rate, however, the full length was heated to achieve a reasonably high exit quality.

Measurements

Wall temperature measurement. The heat transfer coefficient determined in this work is defined as:

$$h = \frac{(Q/A)}{(T_w - T_f)} \tag{1}$$

The outside wall temperature on the heated tube was measured by 30-gauge copper-constantan thermocouples initially mounted in 17 stations and later in 25 stations. There have been many ways of attaching wall thermocouples to the tube, such as spot-welding [4] and brazing [10]. These methods, however, may alter the original characteristics of thermocouples, since high temperature is required to make junctions and attach them to the wall. To avoid any deterioration of thermocouples, all wall thermocouple junctions were soft-soldered with a 50% Pb/50% Sn solder and attached to the tube by mechanically clamping them as was done by Ross et al. [5].

Each station had four thermocouples whose junctions were flattened and polished

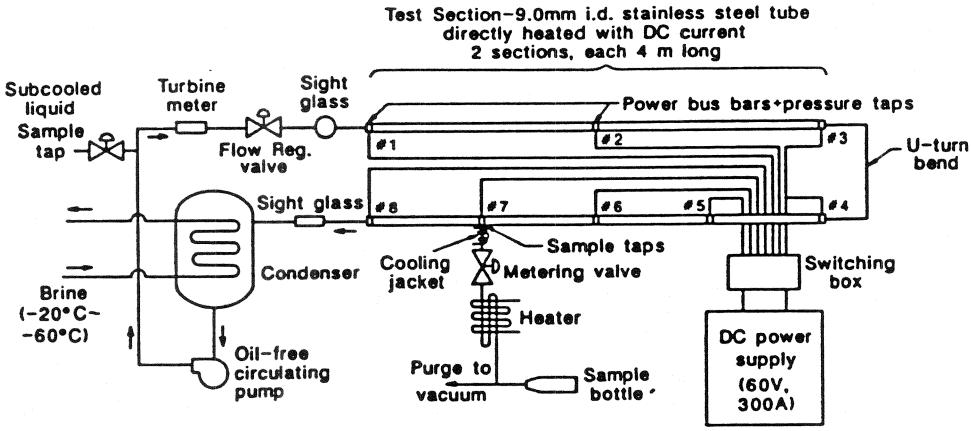

Fig. 1 Schematic diagram of experimental apparatus.

for good thermal contact. They were clamped to the top, both sides, and bottom of the tube by using plastic bushings with cable ties. The thermocouples were electrically insulated from the tube by a layer of PTFE (Teflon) tape. All of the thermocouples were referenced to a refrigerated ice bath whose precision is ±0.02°C. The use of this ice bath reduced uncertainties regarding the quality of a slush ice bath. Actual signals to the voltmeter were converted to temperatures by the method described in an NBS monograph. The fourth-order curve fit used has a maximum error of ±0.02°C over the temperature range −40 to 130°C against the data in [11].

Pressure measurement. Two types of fluid temperatures, T_f in Eq. (1), have been used among the previous experiments: a measured bulk liquid temperature, T_b [7], and a calculated saturation temperature corresponding to the pressure at the wall thermocouple station, T_{sat} [3–5]. The first approach of measuring the bulk liquid temperature is rarely used, since the insertion of instream thermocouples near the wall thermocouple station would alter the flow pattern and consequently the heat transfer coefficient. Besides this, design engineers usually would know the pressure, not the bulk liquid temperature, at a certain point in a heat exchanger, and thus the heat transfer coefficients based on the saturation temperature would be more useful for design purposes. Based on this argument, the second approach of using the calculated saturation temperature as T_f was adopted in this study.

Figure 2 illustrates a detailed diagram for the pressure and sampling taps soldered on the power bus connection (#2, #5, #6, and #7 in Fig. 1). There, however, is only one port at the top for pressure measurement in the bus connections at inlet and outlet of the test section and before and after the U-turn bend (#1, #3, #4, and #8 in Fig. 1). Fine holes (<0.5 mm) were machined through the 0.25-mm-thick stainless steel test section by electrical discharge machining (or spark erosion) to ensure a smooth, burr-free inner surface. A 3.1-mm-o.d. stainless steel tube was silver-soldered on a copper bushing (18.8 mm wide, 9.4 mm i.d., and 15.6 mm o.d.), which was, in turn, soft-soldered to the copper strip that served as a power cable connection. The pressure lines were electrically isolated from the test section by using plastic bushings over a copper tube as in Fig. 2.

Four pressure transducers and one differential pressure transducer in conjunction

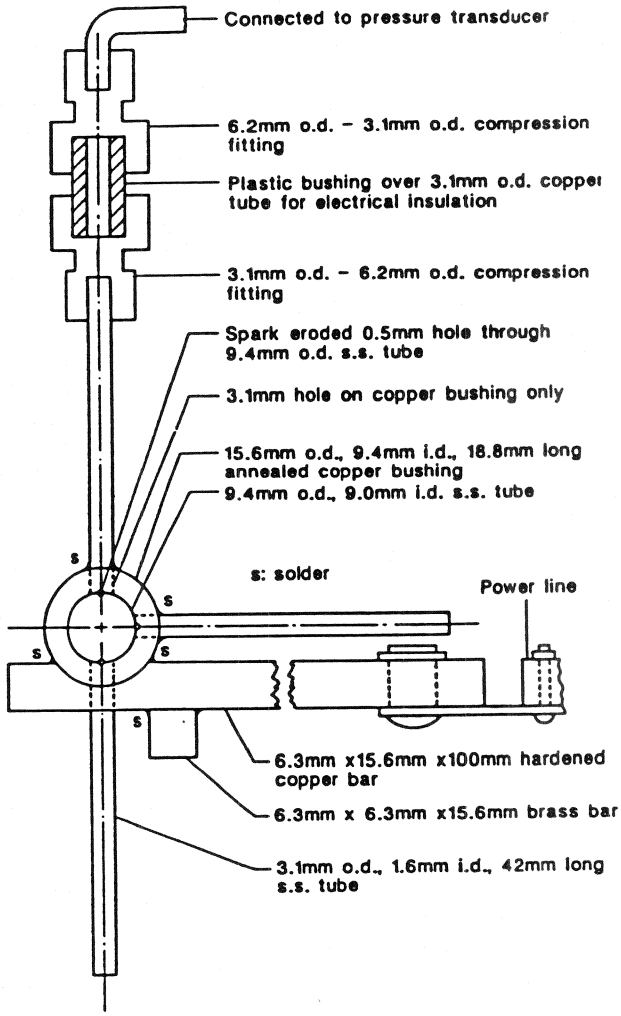

Fig. 2 Diagram of pressure and sampling taps.

with two five-way valves were used for the pressure measurements at eight bus connections. Two presure transducers (0–3447 kPa, abs. pressure) were fixed at the inlet and outlet of the test section (#1 and #8 in Fig. 1). Pressures at points 2 and 3 were measured by another pressure transducer 0–3447 kPa, abs. pressure) with the aid of the five-way valve. The differential pressure transducer (0–69 kPa, differential pressure), whch was referenced to the outlet pressure, was used to measure the pressure differences between points 4 and 8, 5 and 8, 6 and 8, and 7 and 8 via another five-way valve. With these pressure drops and absolute pressures at points 4 and 8, pressures at points 5, 6, and 7 were determined. All absolute pressure transducers were calibrated using a dead-weight pressure tester three times over 18 months. They drifted less than ± 3 kPa.

Given these pressures at eight locations, the local pressures at the thermocouple locations still needed to be estimated. In the subcooled, single-phase flow regime, a

single-phase pressure correlation [12] was applied to calculate the pressure drop from the inlet to the saturation point; the local pressures in this range were linearly interpolated. Beyond the saturation point the local pressures were linearly interpolated from the known pressure values at the adjacent pressure taps.

Mass flow rate measurement. A turbine meter was installed in the subcooled liquid line about 80 diameters upstream of the test section inlet as shown in Fig. 1 to measure the mass flow rate. This measurement was used in conjunction with an energy balance on the test section to determine the specific enthalpy of the refrigerant. The signal (frequency, Hz) from the turbine meter was sent to a pulse counter as well as to a counter integral to the data acquisition system. The readings from these two counters agreed within 1%. The turbine meter was calibrated with tap water at room temperature. It showed a linear response at high flow rates ($\dot{m} > 20$ g/s). The responses at low flow rates disclosed a nonlinearity, and hence many calibration points were obtained at low flow rates. The volume flow rates were interpolated from these calibration points. The mass flow rate was then calculated by multiplying the volume flow rate to the subcooled inlet density, which was calcualted by the CSD equation of state with measured pressure and temperature.

Power measurement. A low-voltage, high-current power supply (60 V DC, 300 A) was used to heat the test section. As mentioned earlier, the heated length of the test section can be varied from 2 to 8 m. This was accomplished with a power switching box containing the positive and negative terminals of the power supply and also a threaded copper post connected to each of the seven bus connections in the test section. By fixing copper connection bars between the power supply and test section connections, only the required portion of the test section could be heated.

Voltage drops across the various segments of the test section and a standard resistor (0.001 Ω), in series with the test section, were measured by the digital voltmeter. The current through the test section was calculated from the voltage drop across the standard resistor, and consequently the total power input to the test section was determined. Early in the testing program, the electrical resistance of the stainless tube was checked and its resistance was shown to be proportional to length, suggesting the absence of local hot spots. The measured voltage drops across the various segments also supported the constancy in resistance with length.

Overall composition measurement. Overall composition for a mixture, C_o, was determined by drawing a subcooled liquid sample from the sampling port in the subcooled liquid line as shown in Figs. 1 and 3. The following procedure was taken for each measurement.

1. Evacuate the sample bottle and connect it to the sampling port.
2. Open valves #1 and #2; evacuate the space between value #1 and the shutoff valve; close valves #1 and #2.
3. Put ice around the sampling line up to the liquid reservoir to avoid flashing.
4. Open valve #1 and shutoff valve consecutively to fill the liquid reservoir.
5. Close valve #1 and shutoff valve and detach the sample bottle from the port.
6. Open valve #2 to expand the subcooled liquid to superheated vapor and run hot water (50–60 °C) over the sample bottle to make certain that no liquid droplets are left.
7. Since the pressure inside the bottle is low (usually below atmospheric pressure),

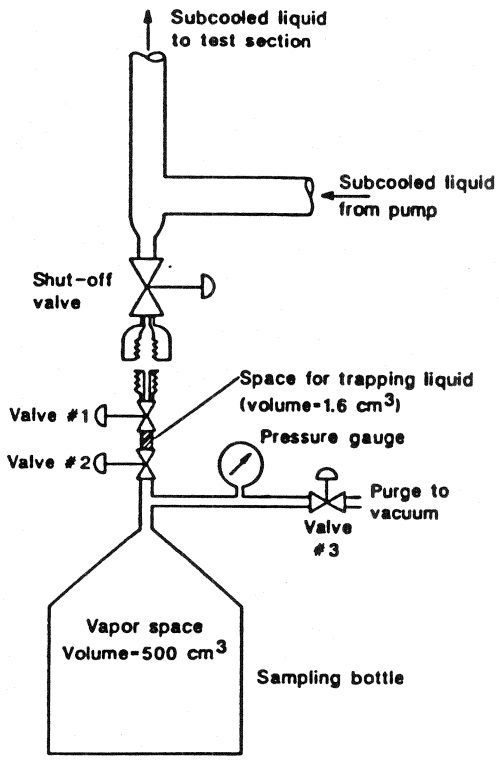

Fig. 3 Diagram for overall composition measurement.

the bottle is pressurized by dry nitrogen to 350 kPa and taken to the gas chromatograph for the composition analysis.

The most important point in the overall composition measurement is to avoid two-phase conditions: the sample should be in single phase always. It is important to make sample bottles large enough to ensure that the sample will be expanded completely to superheated vapor. The addition of a pressure gauge to the sample bottle was another way of checking if the liquid sample had been completely vaporized in the expansion process. If the pressure inside the bottle after the expansion is less than the saturation pressure corresponding to room temperature, then the vapor is presumed to be in the superheated region.

Composition analysis was done by gas chromatography. Each component of a mixture was separated while being carried by helium through a 4-m-long column (Porapak Q, mesh 100–120). A thermal conductivity detector was employed. The reproducibility of the measurement was within 0.2% for the same sample. The variation of composition from sample to sample for the same test was less than 0.5% in mole composition.

Local liquid composition measurement. In order to resolve the issue of whether the circumferential wall temperature variation seen with mixtures [5] is due to a corresponding circumferential composition variation, local liquid film compositions were

measured by drawing samples from the liquid film in annular flow. Three sampling taps, Fig. 2, were made on the top, side, and bottom of the tube in the bus connection located 7 m from the inlet as shown in Fig. 1. A detailed schematic diagram of the local liquid sampling loop is given in Fig. 4. The difficulty of the measurement arises from the fact that only liquid is to be sampled, since the composition of the vapor flowing in the core of the tube is quite different from that for the liquid film.

Double-pattern fine metering valves (0.79-mm-diameter orifice) were used to control the sampling rate. A variety of valve settings were tried initially until further decreases in the valve opening resulted in no change in composition, indicating that only liquid was being sampled. Since the sample was drawn by the pressure difference between the test section and the evacuated sample bottle and since valve settings could not be reproduced accurately, the sample rate changed from test to test. To ensure that no vapor was drawn, the samples were drawn at a further reduced valve opening. Sampling rates through the valve were estimated by measuring the rate of pressure increase in the samping bottle; they were below 0.25 ml/min of liquid. The time required to bring the pressure of the sample bottle from vacuum to an absolute pressure of 75 kPa was usually 2.5 min.

Since the liquid may flash to a vapor before reaching the metering valve and thus affect the flow rate, the valves and the sample lines upstream of the valves were wrapped by a cooling jacket to ensure that only subcooled liquid entered the valve. A separate ethylene glycol flow loop was installed to meet the cooling load in the cooling jacket. After passing through the valve, the liquid was heated to superheated vapor. Samples from the three taps were collected simultaneously. Two sets of samples were taken for each flow condition. The reproductibility of the measurements was within 0.3 mol%.

Data Collection

All tests were run at steady-state conditions. The pressure at the outlet of the test section was kept at a reduced pressure, p_r, of 0.08, which corresponds to 400, 260, 330, and 360 kPa for pure R22, R114, R12, and R152a, respectively. The reduced pressures

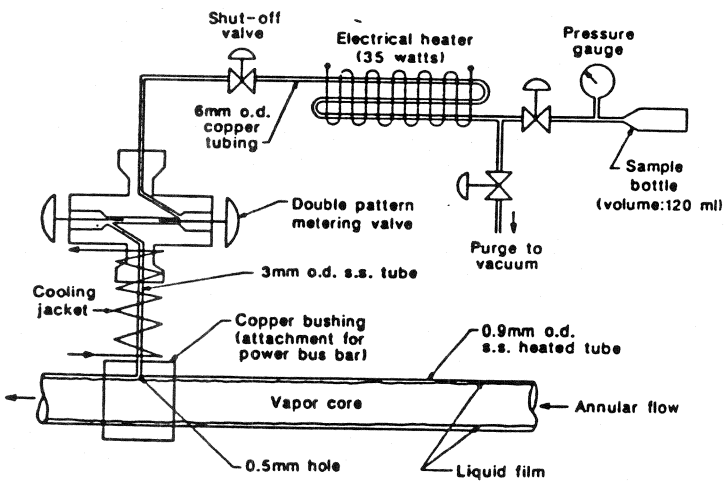

Fig. 4 Diagram for local liquid composition measurement.

for mixtures were determined from the critical pressures calculated by a linear mole fraction weighting (ideal mixing rule) of the pure components' critical pressure values. Due to pressure drops across the test section, however, pressures upstream of the outlet were up to 25% higher than those of the outlet.

Data collection and system control were done by the use of a microcomputer and data acquisition system. A single scan took 90 s to record the following variables: 89 emf values from thermocouples (later 113 emf values due to the eight added thermocouple stations), 8 DC voltages from the bus connections, 1 DC voltage from the standard resistor, 9 DC voltages from the pressure transducers, and a frequency reading from the turbine meter. It usually took 1–2 h for the system to reach steady state, which was indicated by monitoring several key system temperatures and also the sum of the differences between the successive scans of the recorded variables. When steady-state condition was observed for more than 20 scans, those scans were stored and constituted a test.

Data Reduction

The inner wall temperature, T_w, was determined from the measured outside wall temperature via a one-dimensional heat conduction equation assuming uniform heat generation within the tube wall and an adiabatic condition on the outside of the tube. The corrections made by this procedure ranged from 0.08 to 0.32 °C depending on the heat flux.

The fluid temperature, T_f, was calculated rather than directly measured due to the reasons explained earlier. For pure components, the thermodynamic equilibrium temperature (or saturation temperature) corresponding to the pressure was used as T_f at each thermocouple station. For mixtures, however, the thermodynamic equilibrium temperature, T_{eq}, is a function of quality as well as pressure. A local pressure and a specific enthalpy, which are easily measurable quantitites, were used to determine T_f for mixtures. A specific enthalpy at each thermocouple location was determined through an energy balance from the inlet to the particular thermocouple station. Given the pressure, specific enthalpy, and overall composition, the CSD equation of state [6] calculated all thermodynamic properties such as the equilibrium temperature, quality, and liquid- and vapor-phase compositions.

The measurement of wall superheat, $T_w - T_f$ in Eq. (1) to high acuracy put severe requirements on the measurements of local pressure, mass flow rate, and overall composition. For pure components, the accuracy of the wall superheat depended largely on the accuracies of the local pressure measurements (typically 3–4 kPa, corresponding to 0.3–0.4 °C in saturation temperature), wall temperature measurements (0.2 °C), and the CSD equation state (0.2 °C).

For mixtures, besides the uncertainties in the local pressure and wall temperature measurements, the errors in the wall superheat were due to the uncertainties involved in the overall composition measurement (typically 0.5%, corresponding to 0.3 and 0.03 °C in saturation temperature for R22/R114 and R12/R152a mixtures), mass flow rate measurement for the energy balance (1%, corresponding to 0.1 to 0.2 °C in saturation temperature), and finally due to the inaccuracy of the CSD equation of state (0.4 °C). From these uncertainties the most probable errors in the wall superheat were calculated according to the method of Doebelin [13] and were 0.35, 0.4, and 0.67 °C for R22, R114,

and R22/R114 mixtures and 0.4, 0.3, and 0.4°C for R12, R152a, and R12/R152a mixtures.

The heat flux, q, was calculated from the measured power input, calculated heat gain, and internal area of the tube. Even though the test section was well insulated with 200-mm-diameter fiberglass insulation, there was heat gain (or loss) from the surroundings due to the temperature difference between the test section and the surroundings. Heat gain was typically 30 to 40 W, which was less than 3% of the lowest heat input used in the study.

Since the bus connection was made of a heavy copper strip and a bushing soldered to the tube as shown in Fig. 2, the electrical resistance of the bus bar was very small, resulting in virtually no heating in this portion. Thus, 19 mm, the width of the copper bushing, for each 2 m in the first 4-m section and for each 1 m in the last 4-m section was not heated, which corresponded to 1.2% of the total test section length. The uniformity of the tube, confirmed by comparing the voltage drops across each segment between adjacent bus connection, was within 1% deviation. The most probable error in heat flux measurement was determined to be 1.5%.

With these most probable errors in the wall superheat and heat flux, the accuracies of the local heat transfer coefficients in Eq. (1) were determined to be 5–11%, 5–7%, and 5–10% for R22, R114, and their mixtures, respectively, for the quality range 0–70%. For the same quality range, the accuracies for R12/R152a mixtures were 6–10%, 8–14%, and 7–12% for R12, R152a, and their mixtures, respectively. Larger errors occurred at high qualities because of the smaller values of wall superheat, which were typically 3, 5, and 6°C for R122, R114, R122/R114 mixtures and 4, 2.4, and 3°C for R12, R152a, and R12/R152a mixtures at 70% quality.

At each thermocouple station, the average local two-phase flow heat transfer coefficient, h_{tp}, was calculated by

$$h_{tp} = \frac{h_t + h_{ls} + h_{rs} + h_b}{4} \tag{2}$$

Data Verification

Power, instream temperature, and mass flow rate measurements were simultaneously substantiated by an energy balance across the test section. Subcooled pure and mixed refrigerants were passed through the test section under a given heat flux and flow rate. The rise in temperature across the test section, $(T_{out} - T_{in})$, was measured between the inlet and outlet of the test section. The energy gained by the fluid, $\dot{m}C_p(T_{out} - T_{in})$, was compared to the sum of the power input and heat gain from the surroundings. The average of relative errors is less than 2.5%. These energy balance tests were performed over a period of one and a half years. The results indicated that all sensors and the instrumentation have been working correctly.

An indirect confirmation was also obtained by measuring single-phase heat transfer coefficients and comparing these results to existing correlations that have accurately correlated single-phase heat transfer coefficients by other investigators. Five tests for pure refrigerants and eight for mixtures were performed with the subcooled liquid heated throughout the test section. The results were compared to the Dittus-Boelter [14] and

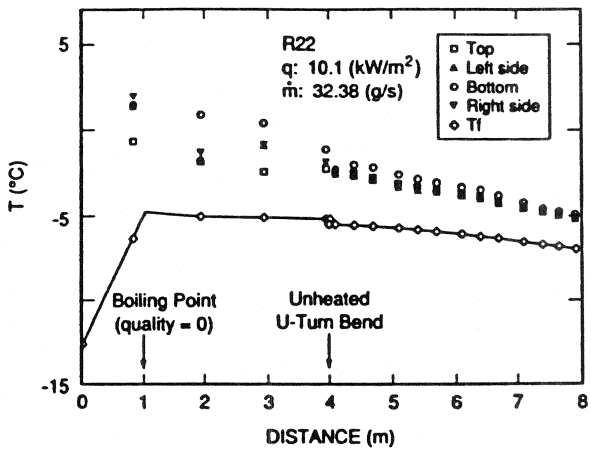

Fig. 5 Wall temperature variation for R22.

Petukhov equations [15]. Both equations correlated the present results with ±5% mean deviation; the two equations differed from each other by less than 2%. Due to the simplicity and popularity of the Dittus-Boelter equation, Eq. (3), the comparison was made with this equation only.

$$h_l = 0.023 \frac{k_l}{d} \left(\frac{Gd}{\mu_l}\right)^{0.8} \left(\frac{C_{pl}\mu_l}{k_l}\right)^{0.4} \tag{3}$$

The good agreement with the accepted correlations of the data taken with the present test facility indirectly substantiated the measurements for the power, mass flow rate, wall temperature, and pressure.

RESULTS AND DISCUSSION

Temperature Measurements

Figures 5 and 6 illustrate the wall temperature variations along the heated tube for pure R22 and 48%R22/52%R114 mixture, respectively. Even though Singal et al. [4] observed large fluctuations in the wall temperatures and attributed this to the instability of two-phase flow, the present results do not show these kind of fluctuations but display very well-defined wall temperature along the channel.

Another point to be noted is that for pure fluids and the mixtures of R12/R152, the wall temperatures at the top of the heated tube are lower than those for the bottom in annular flow. For R22/R114 mixtures, however, the opposite phenomenon is observed. The difference between the temperatures at the top and bottom becomes smaller as quality is increased. This phenomenon of circumferential wall temperature variation is discussed later in this paper. Figure 7 shows the pressure variation along the tube, which is determined by the method described earlier. Pressure drop is shown to increase exponentially as quality is increased.

The fluid temperatures, T_f, determined by this pressure measurement are also

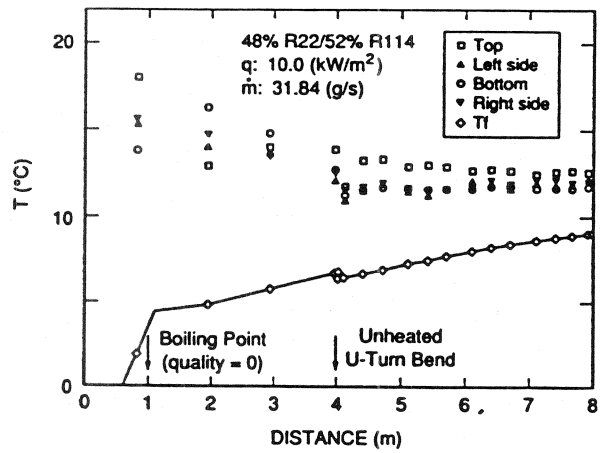

Fig. 6 Wall temperature variation for 48% R2/52% R114 mixture.

shown in Figs. 5 and 6. For pure fluids, T_f in a saturated region is shown to decrease along the channel due to pressure drop. For mixtures, T_f was found to increase as quality is increased in two-phase region, called a gliding temperature effect. In most technical applications where the tube diameter is not extremely small and thus pressure drop is not too large, the gliding temperature effect wins over the temperature decrease due to pressure drop. Consequently, T_f rises along the channel for mixtures as shown in Fig.6.

Overall Composition Measurements

One point to be noted in the overall composition measurement is that the overall compositions of the refrigerant circulated throughout the test section differed from the initially charged composition by 2–3% and 0.5% in mole fraction for the R22/R114 and R12/R152a mixtures. This depended on how much vapor was generated in the system. When heat was not applied and subcooled liquid was circulated throughout the test

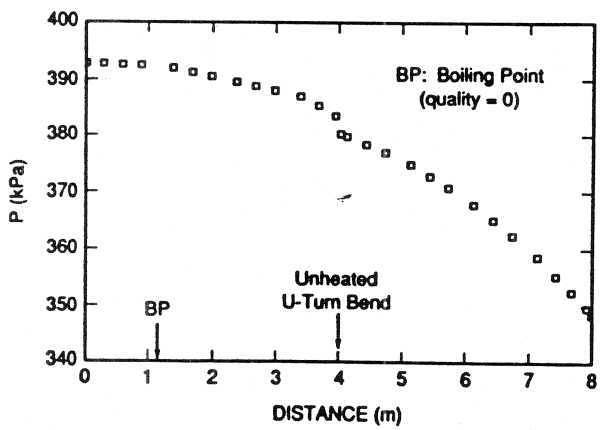

Fig. 7 Pressure variation for R22.

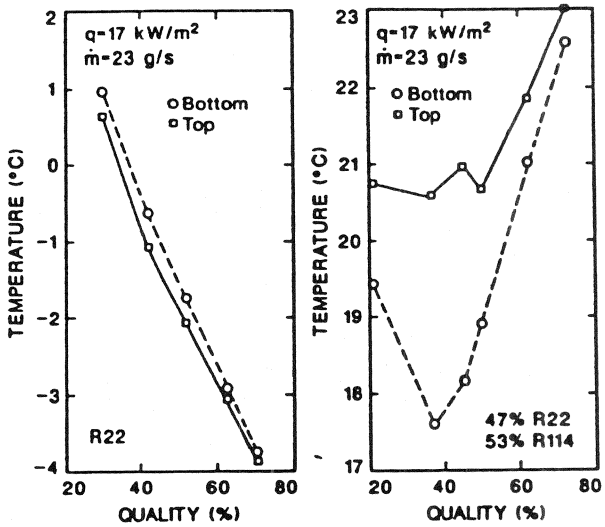

Fig. 8 Circumferential wall temperature variation for R22/R114 mixture.

section, the overall composition was identical to the initially charged composition. When heat was applied, however, the overall compositions were shifted toward the less volatile component.

At first, a leak in the system was suspected but none was found. In fact, since the vapor generated by heating was enriched in the more volatile component, there was a composition shift in the remaining liquid toward the less volatile component. This phenomenon was observed for both nonazeotropic R22/R114 and azeotropic R12/R152a mixtures. The magnitude of the overall composition shift for the R12/R152a mixture, however, was much smaller than that for R22/R114 because of the lesser volatility difference between R12 and R152a as compared to R22 and R114. For the azeotrope (R500, 60% R12/40% R152a), there was no shift in the overall composition as expected.

This finding contradicts the assumption made by Singal et al. [4] and Ross et al. [5] that the overall composition of the liquid entering the test section is the same as the initially charged composition throughout the tests. This assumption artificially lowers the saturation temperature of mixtures by up to 2°C, resulting in lowering the heat transfer coefficients of mixtures by up to 25%, considering that a typical wall superheat, $T_w - T_f$, was 3–8°C. Thus, it is recommended that a liquid sample be drawn and analyzed for each mixture test.

Local Liquid Composition Measurements

Figure 8 illustrates wall temperatures profile versus quality for pure R22 and 47% R22/53% R114 mixture for the same flow condition. Since the quality is over 20%, an annular flow pattern is assumed. For pure components, the temperature at the bottom is higher than at the top by 0.1 to 0.3°C. For R22/R114 mixtures, however, the temperature at the bottom is lower than at the top by as much as 4°C at low qualitities, with

smaller differences at higher qualities. Figure 9 shows the heat transfer coefficients calculated by the method presented above for pure and mixed refrigerants of R22 and R114 for the same flow condition. The coefficients at the top are severely degraded with R22/R114 mixtures. For R12/R152a mixtures, however, the wall temperatures did not show the trend of R22/R114 mixtures but behaved in the same way as pure fluids.

Local liquid film composition measurements were conducted to explore this unique behavior of mixtures for two sets of flow conditions at several qualities. Figure 10 shows the measured overall and local liquid compositions and the average equilibrium liquid compositions calculated by the CSD equation of state [6] based on measured pressures, specific enthalpies, and overall compositions. As seen in Fig. 10, the locally measured compositions at the top are always lower in the more volatile component than the ones at the bottom except for test 4. For this test, the quality at the sampling port was 82% and local dry-out may have been present at the top so that vapor was drawn with the sample.

The equilibrium compositions calculated by the CSD equation of state fall between the measured values for the top and bottom and are close to those for the side. The present results show a circumferential composition variation as alrge as 0.07 mole fraction R22 at relatively low qualities, with smaller composition differences at higher qualities. Thus, R22/R114 mixtures are not fully mixed circumferentially. The top is richer in the less volatile component, R114, and the bottom is richer in the more volatile component, R22. This result confirms the conjecture by Ross et al. [5] that there might be a circumferential composition difference. The same measurements were taken for R12/R152a mixtures under similar test conditions. The results, however, did not indicate a circumferential composition variation. Thus, this mixtures does not show the wall temperature variation as with pure fluids.

The cause for the circumferential variation of composition may be explained as follows. Since the heat flux is uniform, the rate of vapor generation will also be uniform. But the liquid film at the top is thinner due to gravity; thus, evaporating vapor (enriched in the more volatile component) at a constant rate will cause the remaining liquid at the top to shift in composition toward the less volatile component more rapidly than at the bottom. This is due simply to the requirements of a mass and species balance.

The existence of significant circumferential composition variation implies that there may be a relatively little top-to-bottom mixing. At higher qualities, the composition of the liquid film is seen to be nearly uniform circumferentially. This may be due to the lessened influence of gravity with the thinner liquid film and higher vapor velocity at high qualities or perhaps to a more rapid equilibration between the liquid and vapor.

As a result of this composition variation, the local equilibrium temperatures are different circumferentially. This result explains why heat transfer coefficients at the bottom are higher than at the top in an annular flow regime for mixtures. In calculating heat transfer coefficients for mixtures, Eq. (1) has been used by Ross et al. [5] and so far in this study with the assumptions that both phases are in equilibrium and that the composition of each phase is uniform over a given cross section of the heated tube. The results from local liquid composition measurements, however, indicate that at least the latter assumption is not valid. Actual local heat transfer coefficients for mixtures may be obtained by using local equilibrium temperatures, T_{eq}, which are calculated by the equation of state given a measured pressure and a measured liquid composition.

Table 1 lists heat transfer coefficients calculated by two sets of fluid temperatures;

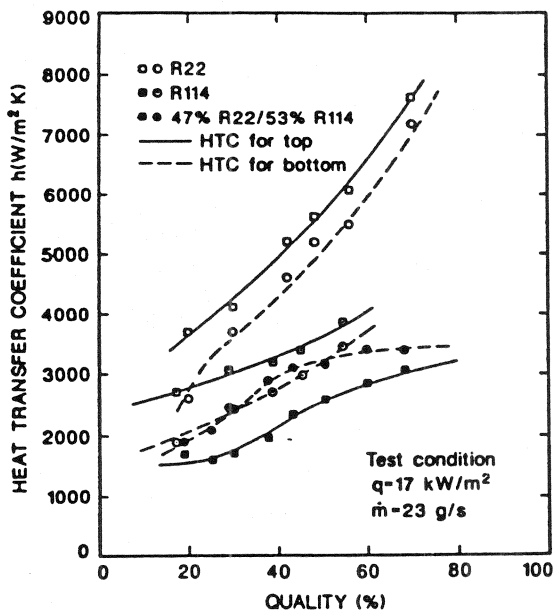

Fig. 9 Circumferential heat transfer coefficient variation for R22/R114 mixture.

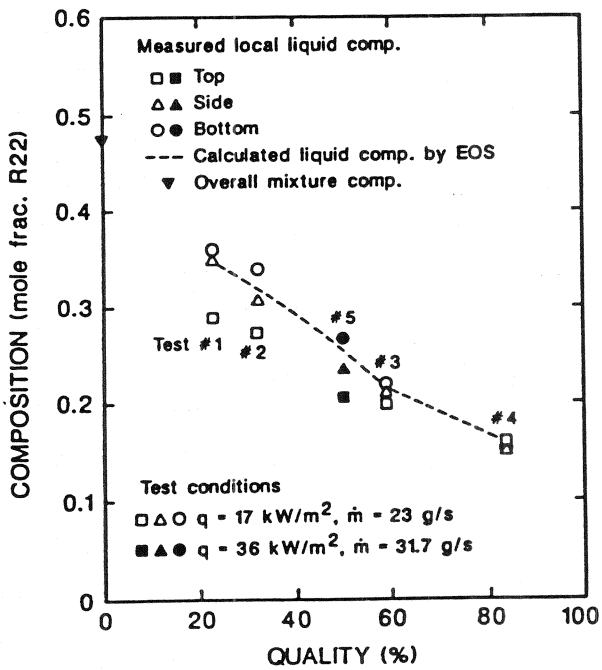

Fig. 10 Comparison between the measured and calculated liquid compositions.

Table 1 Comparison of the Measured Liquid Compositions and Calculated Ones by Equation of State and Heat Transfer Coefficients Calculated by Two Method

Test no.	Location	Meas. local liquid comp. C_l	Local equilibrium fluid temp. baesd on C_l T_{eql} (°C)	Cal. average fluid temp. by EOS $T_{eq}a$ (°C)	Meas. wall temperature T_w (°C)	HTC based on T_{eql} h_{eql} (W/m^2 K)	HTC based on T_{eqa} h_{eqa} (W/m^2 K)
1	*t*	0.29	10.04	18.8	1946	1393	
	s	0.35	6.49		16.57	1697	1708
	b	0.36	5.95		16.81	1575	1667
	av			6.55		1728	1619
2	*t*	0.273	11.72		17.4	3019	1942
	s	0.309	9.4		15.0	3062	2681
	b	0.341	7.52		13.8	2740	2580
	av			8.56		2971	2649
3	*t*	0.2	16.84		21.41	3761	27.65
	s 0.21	16.0		20.68	3673	3138	
	b	0.218	15.38		20.05	3680	3138
	av			15.20		3697	3147
4	*t*	0.162	18.49		23.66	3280	3079
	s	0.151	19.51		23.46	4292	3200
b	0.152	19.41		23.19	4485	3368	
	av			18.15		4087	3212
5	*t*	0.206	17.44		25.51	4423	2982
	s	0.235	15.19		23.52	4284	3581
	b	0.266	13.0		21.11	4401	4714
	av			13.54		4424	3714

T_{eqa} and T_{eql}. T_{eqa} is the average saturation temperature in a cross section, which is calculated with a given overall composition. T_{eql}, however, is the local saturation temperature corresponding to the measured local liquid compositions at the top, side, and bottom of the tube. It is seen from Table 1 that when the local equilibrium fluid temperature, T_{eql}, is used in calculating the heat transfer coefficient, the heat transfer coefficients at the top are actually greater than at the bottom even with mixtures. This is the behavior observed with pure components in an annular flow regime and is reasonable since the hydrodynamics of mixtures and pure components should be similar.

Another fact to be noted is that the average heat transfer coefficients based on local equilibrium fluid temperatures show a 10% increase as compared to the heat transfer coefficients based on average equilibrium fluid temperatures. This indicates that a portion of the degradation of heat transfer observed with mixtures may be an artifact of how the heat transfer coefficient is calculated. If this were to be true, the heat transfer degradation with mixtures due to mass transfer resistance (less than 10% of the total heat transfer) would be compensated by using the true local saturation temperature in calculating heat transfer coefficient. Since the measurement of local liquid compositions at each thermocouple location to determine the true local saturation temperature would require a huge effort, the conventional approach to calculate the heat transfer coefficients for mixtures based on an average equilibrium fluid temperature, T_{eqa}, has been preferred throughout this study. Alto, this approach is the one most likely to be used in heat exchanger design.

CONCLUSIONS

The following conclusions can be drawn based on the present experimental flow boiling heat transfer study.

1. Accurate wall temperature and pressure measurements are essential to obtain reliable data. Fluid temperature, T_f, based on measured pressures are recommended to determine heat transfer coefficient. Frequent calibrations of pressure transducers are recommended.
2. The overall composition of the liquid entering the test section should be measured for each test. The assumption that the initially charged composition is the same throughout the tests would artificially lower the heat transfer coefficient of mixtures up to 25%.
3. For the R22/R114 mixture, circumferential composition variations of up to 0.07 in mole fraction are measured for the liquid film in annular flow. This caused a corresponding circumferential wall temperature variation with the R22/R114 mixture. For the R12/R152a mixture, neither phenomenon was observed, suggesting that the mixtures with small differences in liquid and vapor compositions would not reveal the circumferential wall temperature and composition variations.

REFERENCES

1. K. Stephan, Heat Transfer in Boiling of Mixtures, Proc. 7th Int. Heat Transfer Conf., Munich, Paper RK14, 1982.

2. M. Kauffeld, W. Mulroy, M. McLinden, and D. Didion. An Experimental Evaluation of Two Nonazeotropic Refrigerant Mixtures in a Water-to-Water, Breadboard Heat Pump, NBSIR, to be published, NBS, Gaithersburg, Md.
3. D. B. R. Kenning and G. F. Hewitt, Boiling Heat Transfer in the Annular Flow Regime, Proc. 8th Int. Heat Transfer Conf., San Francisco, 1986.
4. L. C. Singal, C. P. Sharma, and H. K. Varma, Experimental Heat Transfer Coefficient for Binary Refrigerant Mixtures of R-13 and R12, *ASHRAE Trans.*, pp. 175–188, 1983.
5. H. Ross, R. Radermacher, M. di Marzo, and D. Didion, Horizontal Flow Boiling of Pure and Mixed Refrigerants, *Int. J. Heat Mass Transfer* vol.30, no. 5, pp. 979–992, 1987.
6. G. Morrison and M. McLinden, Application of a Hard Sphere Equation of State to Refrigerants and Refrigerant Mixtures, NBS Technical Note 1226, NBS, Gaithersburg, Md. 1986.
7. D. L. Bennett, A Study of Internal Forced Convective Boiling Heat Transfer for Binary Mixtures, Ph.D. thesis, Lehigh Univ., Lehigh, Pa., 1976.
8. D. S. Jung, M. McLinden, R. Radermacher, and D. Didion. Horizontal Flow Boiling Heat Transfer Experiments with a Mixture of R22/R114, *Int. J. Heat Mass Transfer*, vol. 32, pp. 131–145, 1989.
9. D. S. Jung, Mixture Effects on Horizontal Convective Boiling Heat Transfer, Ph.D. thesis, Dept. of Mech. Eng., Univ. of Maryland, College Park, Md. May 1988.
10. D. Sachs and R. A. K. Long. A Correlation for Heat Transfer in Saturated Two-Phase Flow with Visualization, *Int. J. Heat Mass Transfer*, vol. 2., pp. 223–230, 1961.
11. R. Powell, W. Hall, C. Hyink, and L. Sparks, Thermocouple Reference Tables Based on the IPTS-68, NBS Monograph 125, NBS, Gaithersburg, Md. 1974.
12. J. G. Collier, *Convective Boiling and Condensation*, 2d ed., McGraw-Hill, New York, 1981.
13. E. O. Doebelin, *Measurement Systems*, rev. ed., McGraw-Hill, New York, 1975.
14. F. W. Dittus and L. M. K Boelter, *Publ. Eng.*, Vol. 2, pp. 443, Univ. of California at Berkeley, 1930.
15. B. S. Petukhov, Heat Transfer and Friction in Turbulent Pipe Flow, in *Advances in Heat Transfer*, vol. 6, pp. 504–564, Academic Press, New York, 1970.